

NASA Technical Memorandum 83116

Holographic Flow Visualization at the Langley Expansion Tube

William K. Goad and Alpheus W. Burner

JUNE 1981

NASA

NASA Technical Memorandum 83116

Holographic Flow Visualization at the Langley Expansion Tube

William K. Goad and Alpheus W. Burner
Langley Research Center
Hampton, Virginia



National Aeronautics
and Space Administration

**Scientific and Technical
Information Branch**

1981

SUMMARY

A holographic system used for flow visualization at the Langley Expansion Tube is described. A ruby laser which can be singly or doubly pulsed during the short run time of less than 300 μ s is used as the light source. Holographic recording of the flow field about a model is especially useful for the low-density flow of the expansion tube. With holography, sensitivity adjustments can be optimized after a run instead of before a run as with conventional flow-visualization techniques. This results in an increase in reliability of the flow visualization available for the study of real-gas effects on flow about models of proposed planetary-entry vehicles. The experimental arrangement and a number of shadowgraphs, schlierens, and interferograms are presented for several test gases and for cases for which the expansion tube was run as a shock tube.

INTRODUCTION

The Langley Expansion Tube is a unique facility providing hypersonic-hypervelocity flow for typical run times of several hundred microseconds. Low free-stream densities at the facility make optical flow visualization marginal despite relatively high density ratios across the normal shock. As discussed in reference 1, a primary measurement made in the expansion tube is the shock shape about a model. When standard flow-visualization techniques (ref. 1) are used, it is impossible either to optimize adjustments during the run because of the short run time, or to assure that prerun settings will prevail during the run.

If holography is used to optically record the flow field, sensitivity adjustments in the flow-visualization system can be made after the run while reconstructing the hologram. Also several different techniques for flow visualization can be tried using a single hologram to determine which technique best depicts the flow. Another advantage of holography is its ability to provide interferometry with little extra effort, therefore providing a more versatile system. With interferometry, either density measurements can be made or a comparison of experimental and theoretical interferograms can be used to verify mathematical models of the flow field. Because of these advantages over a conventional flow-visualization system, a holographic system was installed at the Langley Expansion Tube. The purpose of this report is to describe this holographic system and to present results obtained with the system during the various tests in both the expansion-tube and shock-tube modes of operation.

Use of trade names or names of manufacturers in this report does not constitute an official endorsement of such products or manufacturers, either expressed or implied, by the National Aeronautics and Space Administration.

SYMBOLS

M	Mach number
U	velocity, m/s
ϵ	normal shock density ratio, ρ_2/ρ_∞ or ρ_2/ρ_1
ρ	density, kg/m ³

Subscripts:

s	incident shock
1	state of quiescent test gas in front of incident shock
2	state of test gas immediately behind incident shock or standing at the model
∞	free-stream conditions

FACILITY DESCRIPTION

The Langley Expansion Tube is basically a cylindrical tube divided by two diaphragms (primary and secondary) into three sections. The upstream section is the driver, or high-pressure, section. This section is pressurized at ambient temperature with a gas having a high speed of sound. Greater operation efficiency is realized as driver-gas speed of sound increases. The intermediate section is sometimes referred to as the driven section. This section is evacuated and filled with the desired test gas at ambient temperature. The driver and intermediate sections are separated by double diaphragms. The downstream section is referred to as the acceleration, or expansion, section. A weak, low-pressure diaphragm (secondary diaphragm) separates the driven and acceleration sections. Test models are positioned at the exit of the acceleration section. Flow through this section exhausts into a dump tank; hence, models are tested in an open jet. A detailed description of the basic components and auxiliary equipment of the Langley Expansion Tube is presented in reference 2.

Briefly, the operating sequence for the expansion tube, which is shown schematically in figure 1, begins with rupture of the high-pressure primary diaphragm. In the double-diaphragm mode of operation, this is achieved by pressurizing the driver section and double-diaphragm section with the driver gas to a pressure somewhat less than the rupture pressure for a single diaphragm. The double-diaphragm section is then isolated from the driver section and high-pressure supply field and the driver section is pressurized to the desired pressure. The double-diaphragm section is then vented to atmospheric pressure, resulting in the rupture of the upstream diaphragm. Upon rupture of this diaphragm, the downstream diaphragm is subjected to a pressure essentially that of the driver section. This pressure ruptures the downstream diaphragm, and an incident shock wave is propagated into the arbitrary test gas. The shock wave then encounters and ruptures the low-pressure secondary diaphragm.

A secondary incident shock wave propagates into the low-pressure acceleration gas, while an upstream expansion wave moves into the test gas. In passing through this upstream expansion wave, which is being washed downstream since the shock-heated test gas is supersonic, the test gas undergoes an isentropic unsteady expansion resulting in an increase in the flow velocity and Mach number. Thus, the expansion tube provides hypersonic-hypervelocity flow over a wide range of normal shock density ratios (ref. 1). By removing the secondary diaphragm this facility can be operated as a conventional shock tube (see fig. 1) providing hypervelocity-supersonic flow. A detailed analysis of expansion-tube flow characteristics is presented in reference 3 and in reference 4 with the facility operated as a shock tube.

For the present tests the driver section was 2.44 m long and was 16.51 cm in diameter. Double-diaphragm mode of operation was employed to reduce randomness in pressure ratio across the primary diaphragm at time of rupture. The volume of the section between the double diaphragms was small compared with that of the driver section, with the ratio of double-diaphragm-section volume to driver-section volume being 0.07. Intermediate-section length was 7.49 m and acceleration-section length was 14.13 m. The inside diameter of these two sections was 15.24 cm. The primary diaphragms were stainless steel and the secondary diaphragm was Mylar.¹

The driver gas used in the present study was helium and ranged in pressure from 7 to 34 MPa. Test gases included air, helium, nitrogen, argon, neon, and carbon dioxide. Test-gas quiescent pressures in the intermediate section of the expansion tube or driven section of the shock tube ranged from 69 to 6900 Pa; the corresponding range of shock velocities was 1500 to 5500 m/s. The usable test core for the expansion tube is 7.6 to 8.9 cm in diameter; hence, relatively small models are tested in the facility, typically 5.0 cm in diameter. Models are mounted in a fixed position prior to the run, typically no farther from the exit of the tube than 6.0 cm. Steady flow exists for approximately 300 μ s in the expansion tube, with approximately 10 to 80 μ s required to establish flow over the model as discussed in reference 5, depending upon the test gas, model size, and model geometry.

HOLOGRAPHIC SYSTEM

The holographic system (fig. 2) is similar to that of reference 6 and is discussed briefly in reference 7. The off-axis Z-configuration common to schlieren-photography systems is used to direct the 40-cm-diameter scene beam through the test section. A reference beam which passes over the tunnel intersects the scene beam at the hologram plane to form the holographic recording. A ruby laser, which can be operated in a single- or double-pulse mode with 10 to 500 μ s between pulses, is used to expose the hologram. The path length from the ruby laser to the hologram plane is 18 m.

The ruby and helium-neon alignment lasers are mounted on a large stationary table held firmly in place with approximately 500 kg of lead bricks. The holo-

¹Mylar: Registered trademark of E. I. du Pont de Nemours & Co., Inc.

gram holder is mounted on the opposite side of the test section on an aluminum table anchored to a 65-cm-thick reinforced-concrete wall. Overhead reference-beam optics on the laser side of the system are suspended from 50-cm by 16-cm steel ceiling beams with 10-cm aluminum angles. Simple, stable mounts fabricated at Langley Research Center and having locking adjustments are used for fine positioning of the folding mirrors. All aluminum angles used on the hologram side to support the remaining overhead reference beam optics are anchored to the concrete wall. The stability of this arrangement is evident in that major realignment of the interferometer has been necessary only once during the first year of operation. The need for axial movement in the system of reference 6 required suspension of the entire system from one large overhead beam which proved less stable than the expansion-tube system.

Tunnel windows used for viewing the flow phenomena are bonded three-layer (crown glass-HERCULITE-HERCULITE²) schlieren-grade quality having a slight wedge. They are 8.2 cm thick with a diameter of 40.0 cm. Localized regions of birefringence due to tempering reduces hologram efficiency at the edge of the windows. Usually the hologram reconstructions are sufficiently bright for viewing over an area larger than that required for the small regions of interest in the test section (i.e., 15.2 cm high and 20.3 cm long).

The two-plate hologram holder used for recordings is a commercial unit having a fixed spacing of 0.7 cm between the two plates. The plate position closest to the test section is used for the flow recording. If only a shadowgraph or a schlieren photograph is needed, a no-flow hologram (plate position farthest from the test section) need not be recorded. For hologram reconstructions two separate plate holders were fabricated. One plate can be rotated about three orthogonal axes and the other plate can be translated in three dimensions. With these adjustments the two holograms can be moved with respect to each other to generate an interferogram of desired fringe spacing and orientation.

Reconstructions can be made in place using a 1-W argon-ion laser. A mirror is placed in the reference beam (fig. 3) to direct the argon-laser beam into the expanding and collimating optics used to record the hologram. Broadband multilayer-dielectric coated mirrors are used in the reference beam which have reflectivities of greater than 99 percent for both 694 nm (ruby-laser wavelength) and 515 nm (argon-laser wavelength). Film backs of 10 cm by 13 cm and 20 cm by 25 cm are arranged in a folded configuration to permit varying magnifications and fields of view. The reconstruction laser-beam path is enclosed for safety and ease of operation. Reconstructions can be viewed and photographed with the overhead room lights on. When the daily run frequency precludes using the in-place reconstruction system, a separate lab containing a 50-mW helium-neon laser and a 1-W argon laser is used (fig. 4). This lab is operated for both expansion-tube reconstructions and for recordings made with the system of reference 6.

For comparison, the in-place film backs are also used during some runs to simultaneously record both laser schlieren photographs and holograms. Knife-

²HERCULITE: Registered trademark of PPG Industries, Inc.

edge cutoff and focus are set using the helium-neon alignment laser prior to the run. A narrow-band-pass filter (694 nm) is used in front of high-speed infrared film to prevent radiation emitted during the flow from fogging the film. For certain test gases, severe emissive radiation has been observed at the model when using white-light schlieren photography. The effect of this radiation was reduced with a high-speed capping shutter. For some test conditions this emissive radiation is sufficiently intense to fog even the relatively insensitive holographic plate.

The laser is triggered during each run by a thin-film resistance gage mounted flush with the tube wall. The gage is located 4 m upstream of the tube exit, and thus time is allowed for energy pumping by the laser flash lamp. A digital delay unit is triggered initially by the thin-film gage and in turn triggers the laser and monitoring oscilloscopes (fig. 5). The laser pulse or pulses are detected with a photodiode located at the edge of the scene beam. The photodiode time history is compared with a pressure-transducer time history located close to the model (2.5 cm upstream of the tube exit) to determine the time of laser firings relative to shock arrival at the model. An oscilloscope record illustrating the time-history comparison is presented in figure 6.

RESULTS

The technique used most often at the facility has been two-plate holography. In two-plate holography, separate flow and no-flow holograms are made. By varying the relative position of the two plates during reconstruction the reference-fringe spacing and orientation of the interferograms can be altered. Schlieren photographs and shadowgraphs can be reconstructed from the flow hologram alone.

Simultaneous laser-schlieren and holographic-schlieren recordings for one run of the expansion tube with air as the test gas are shown in figure 7. Figure 7(a) was exposed on high-speed infrared film by the ruby-laser beam after it was slightly attenuated by its passage through the holographic plate. The vertical knife-edge cutoff adjustment was made prior to the run by using the helium-neon alignment laser. Figure 7(b) is the reconstructed schlieren from the holographic plate for which post-run vertical knife-edge cutoff was adjusted to closely duplicate the cutoff used for the laser-schlieren recording. The model is a section of the Space Shuttle Orbiter nose.

Examples of shadowgraphs, schlieren, and interferograms of blunt bodies in the expansion tube with CO₂ as the test gas are shown in figures 8 and 9. For figure 8 the model is a flat-faced cylinder. For figure 9 the model is a spherically blunted 80° half-angle cone with a ratio of nose radius to base radius of 0.5. Holographically reconstructed focused shadowgraphs are shown in figures 8(a) and 9(a). Introduction of vertical knife-edge cutoff produced the schlieren recording of figure 8(b). By using the no-flow holographic plate exposed before each run in addition to the flow plate made during the two runs the infinite-fringe interferograms of figures 8(c) and 9(b) were made. Adjustments of the two plates relative to each other produced the finite-fringe interferograms of figures 8(d), 9(c), and 9(d).

Figures 10 to 14 were recorded during runs when the expansion tube was operated as a shock tube to illustrate the capability of the holographic flow-visualization system. The facility is not normally run as a shock tube for model testing because of the poor flow quality (typical of low-Mach number free-jet test sections), but by increasing the free-stream density, flow fields having large fringe shifts can be represented. An interferometer is sensitive to the difference in density $\Delta\rho$, which for the case of a normal shock in the expansion tube can be expressed as

$$\Delta\rho = (\epsilon - 1)\rho_\infty$$

or for a normal shock in the shock tube as

$$\Delta\rho = (\epsilon - 1)\rho_1$$

where ϵ is the density ratio across the shock, ρ_∞ is the free-stream density, and ρ_1 is the quiescent test-gas density in front of the incident shock. For shock-tube runs in this study the free-stream density is approximately 75 to 125 times greater than for expansion-tube runs. The density ratios across normal shocks in the shock tube were two to three times smaller than for an expansion-tube run, making the density difference across a normal shock much greater for a shock-tube run.

Figure 10 was recorded 100 μs after the shock had exited the tube (tube is on the far left side of photograph) and shows shock-wave propagation (argon test gas) across the test section. Figure 10(a) was reconstructed from the flow plate using vertical knife-edge cutoff, and figure 10(b) is a two-plate interferogram. Figure 11 shows the primary shock after it had passed over a 20° half-angle wedge and before it had left the field of view. Figure 11(a) is a focused shadowgraph made from the flow plate and figure 11(b) is a two-plate interferogram.

Figure 12 shows the primary shock as it exits the tube. This is an example of an interferogram produced by double-pulse holography (both pulses made on the same photographic plate). The first pulse (no flow) fired 150 μs before the second pulse (flow), which occurred 10 μs after the shock exited the tube. The absence of residual fringes demonstrates the "perfect" infinite-fringe capability of the technique. An example of the deviation from a normal shock to a shock with a large curvature is shown by comparing figure 12 with figure 10. The shock radius of curvature in figure 12 is extremely large (essentially normal shock) whereas the radius of curvature for the shock in figure 10 is small (approximately 26 cm) after 120 μs of propagation across the test section.

Figure 13(a) shows the primary shock after it has passed over a spherically blunted 80° half-angle cone with a ratio of nose radius to base radius of 0.5. The initial laser pulse occurred 30 μs before the flow was in the field of view and the second pulse occurred 150 μs after the first pulse, during the flow. Figure 13(b) is an example of double-pulse holography with both laser pulses

occurring during the flow and was obtained at the same flow conditions as figure 13(a). The initial pulse occurred 150 μ s after the flow had exited the tube, with flow on the model for 120 μ s. The second pulse occurred 150 μ s after the initial pulse, when flow had been on the model for 270 μ s. With this rapid double-pulse technique, flow-instability phenomena about blunt bodies can be examined for the time interval established by the pulse separation (150 μ s in this case). Figure 13(a) reveals the strong bow shock expected from high-density flow in a shock tube, and in figure 13(b) two strong bow shocks are shown. The shock standoff distance measured in figure 13(a) is identical to the standoff distance measured in figure 13(b) for the bow shock closest to the model. The change in flow conditions represented in figure 13(b) by the presence of two bow shocks is believed to be due to the arrival of helium driver gas at the model. Figures 14(a) and 14(b) are enlarged photographs of the flow over the lower half of the model from figures 13(a) and 13(b). The enlargements in figure 14 represent 50 \times magnifications of the images stored on the holographic plates and demonstrate the potential for detailed analysis of the flow.

CONCLUDING REMARKS

A holographic system used for flow visualization at the Langley Expansion Tube has been described. This dedicated system has demonstrated greater versatility than the previously used white-light schlieren system by providing laser-schlieren, holographically reconstructed schlieren and shadowgraph, and interferometry. Optimization of sensitivity adjustments provided by the ability to perform these adjustments after the run resulted in a more reliable system than previously used. Holographic techniques such as single-plate schlieren and shadowgraph, two-plate interferometry, double-pulse interferometry for "perfect" infinite-fringe interferograms, and double-pulse interferometry used to examine changes in the flow over a short time period have been described and examples presented.

Langley Research Center
National Aeronautics and Space Administration
Hampton, VA 23665
April 30, 1981

REFERENCES

1. Miller, Charles G., III: Shock Shapes on Blunt Bodies in Hypersonic-Hypervelocity Helium, Air, and CO₂ Flows, and Calibration Results in Langley 6-Inch Expansion Tube. NASA TN D-7800, 1975.
2. Moore, John A.: Description and Initial Operating Performance of the Langley 6-Inch Expansion Tube Using Heated Helium Driver Gas. NASA TM X-3240, 1975.
3. Shinn, Judy L.; and Miller, Charles G., III: Experimental Perfect Gas Study of Expansion-Tube Flow Characteristics. NASA TP-1317, 1978.
4. Miller, Charles G., III; and Jones, Jim J.: Incident Shock-Wave Characteristics in Air, Argon, Carbon Dioxide and Helium in a Shock Tube With Unheated Helium Driver. NASA TN D-8099, 1975.
5. Miller, Charles G.; and Moore, John A.: Flow-Establishment Times for Blunt Bodies in an Expansion Tube. AIAA J., vol. 13, no. 12, Dec. 1975, pp. 1676-1678.
6. Burner, Alpheus W.; and Midden, Raymond E.: Holographic Flow Visualization at the Langley CF₄ Tunnel. NASA TM-74051, 1977.
7. Burner, A. W.; and Goad, W. K.: Holographic Flow Visualization at NASA Langley. Instrumentation in the Aerospace Industry - Volume 25. Advances in Test Measurement - Volume 16, Part Two, Instrum. Soc. America, c.1979, pp. 477-484.

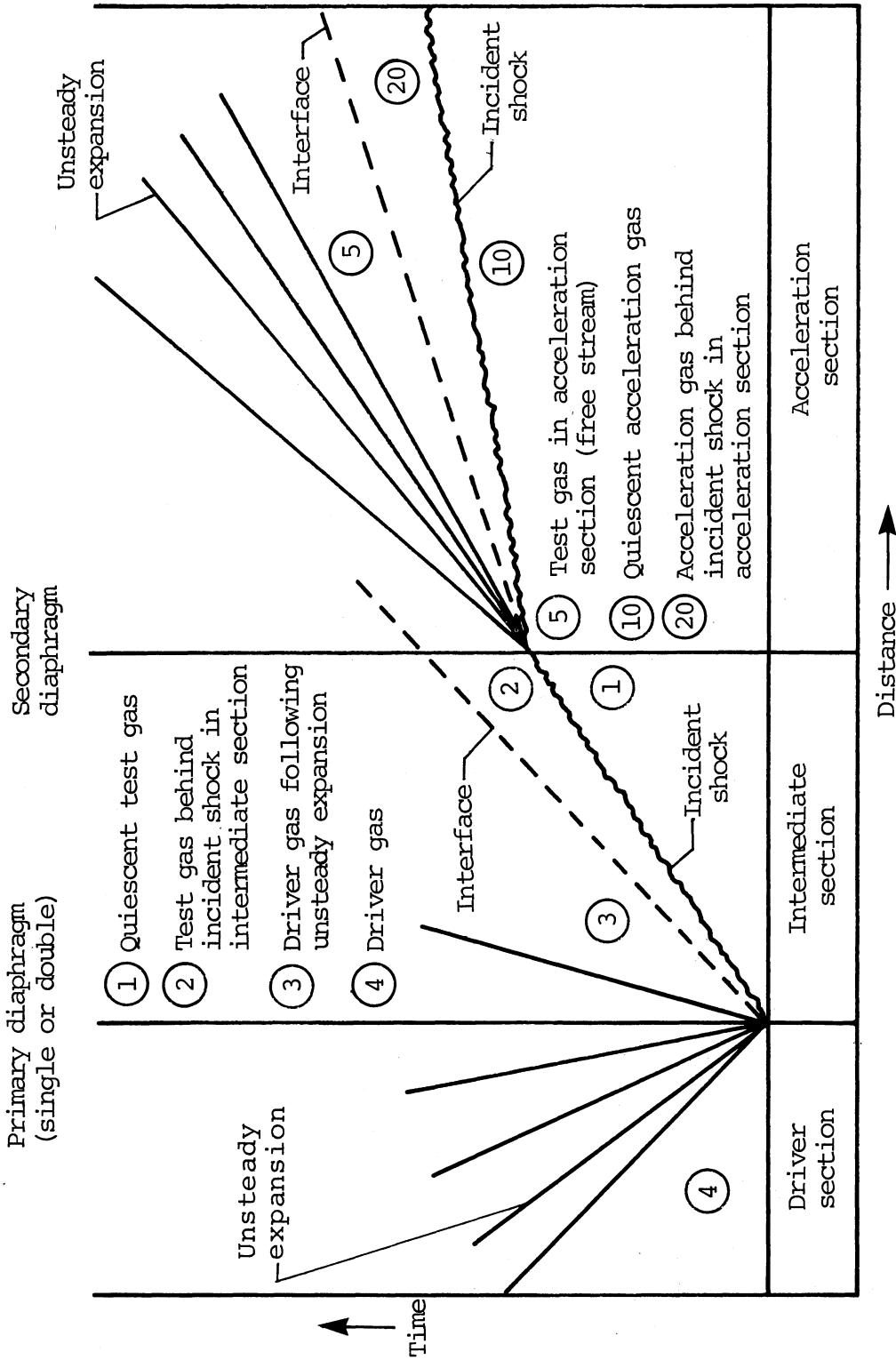


Figure 1.- Schematic diagram of expansion-tube flow sequence.

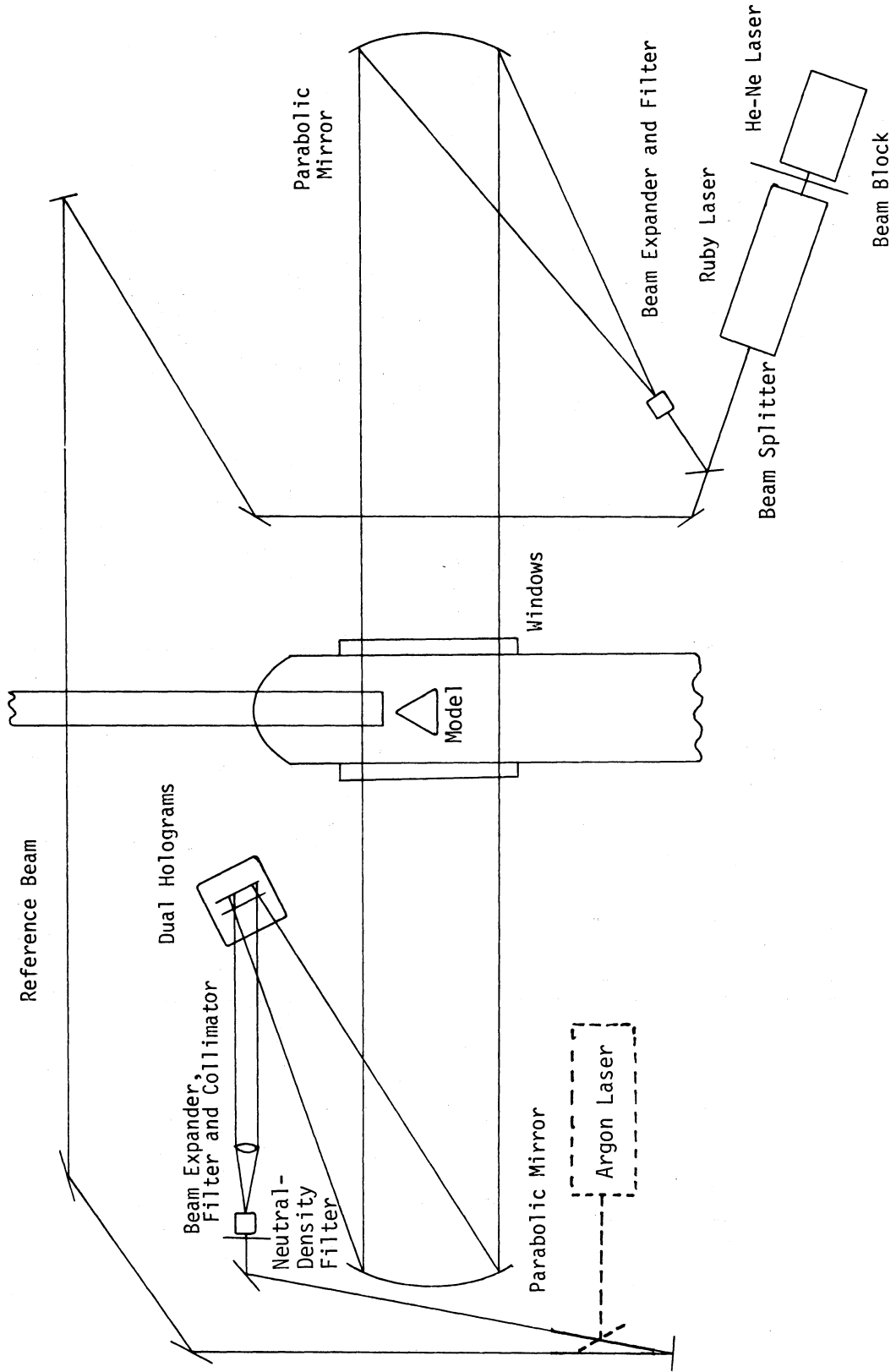


Figure 2.- Pulsed ruby-laser holographic system at expansion tube.

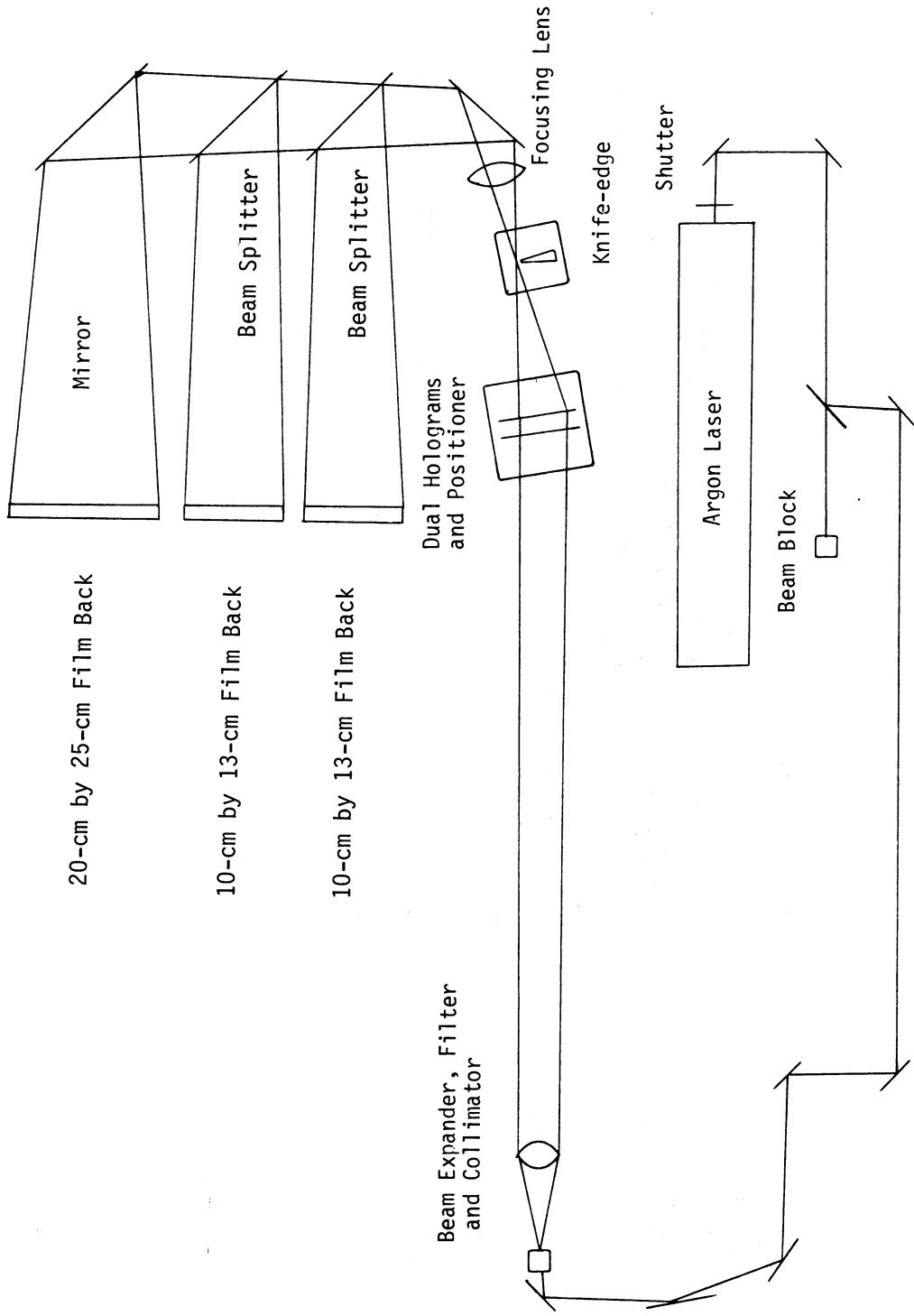


Figure 3.- On-site reconstruction system for expansion tube.

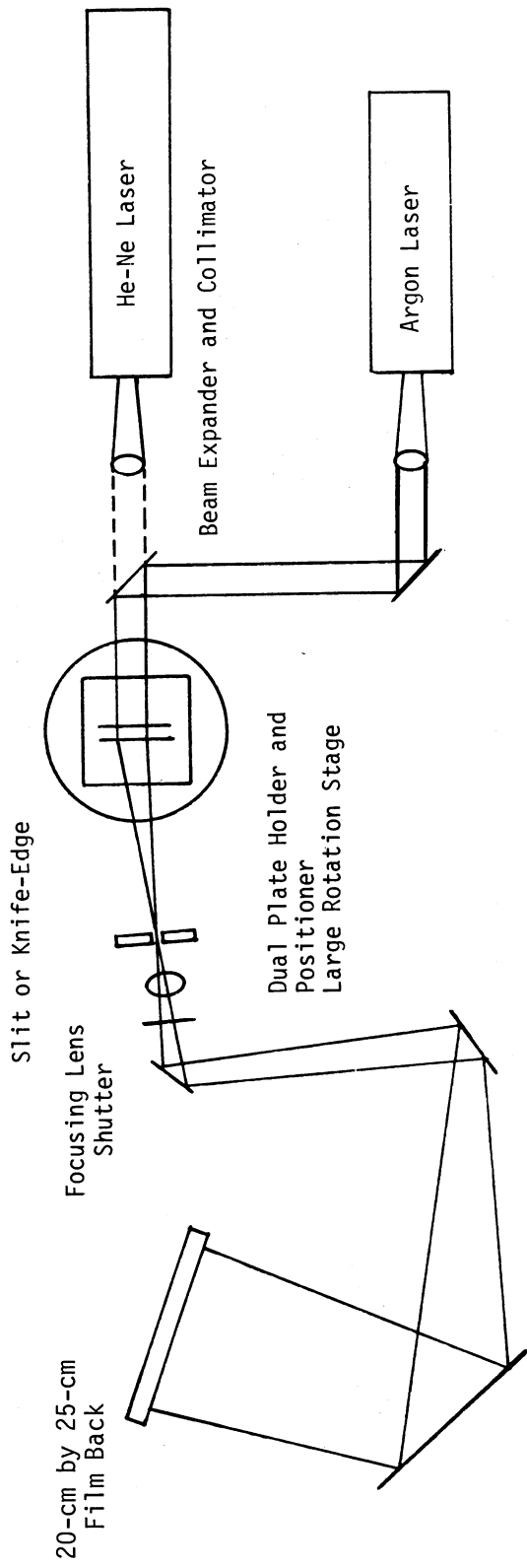


Figure 4.- Off-site reconstruction system for Expansion Tube.

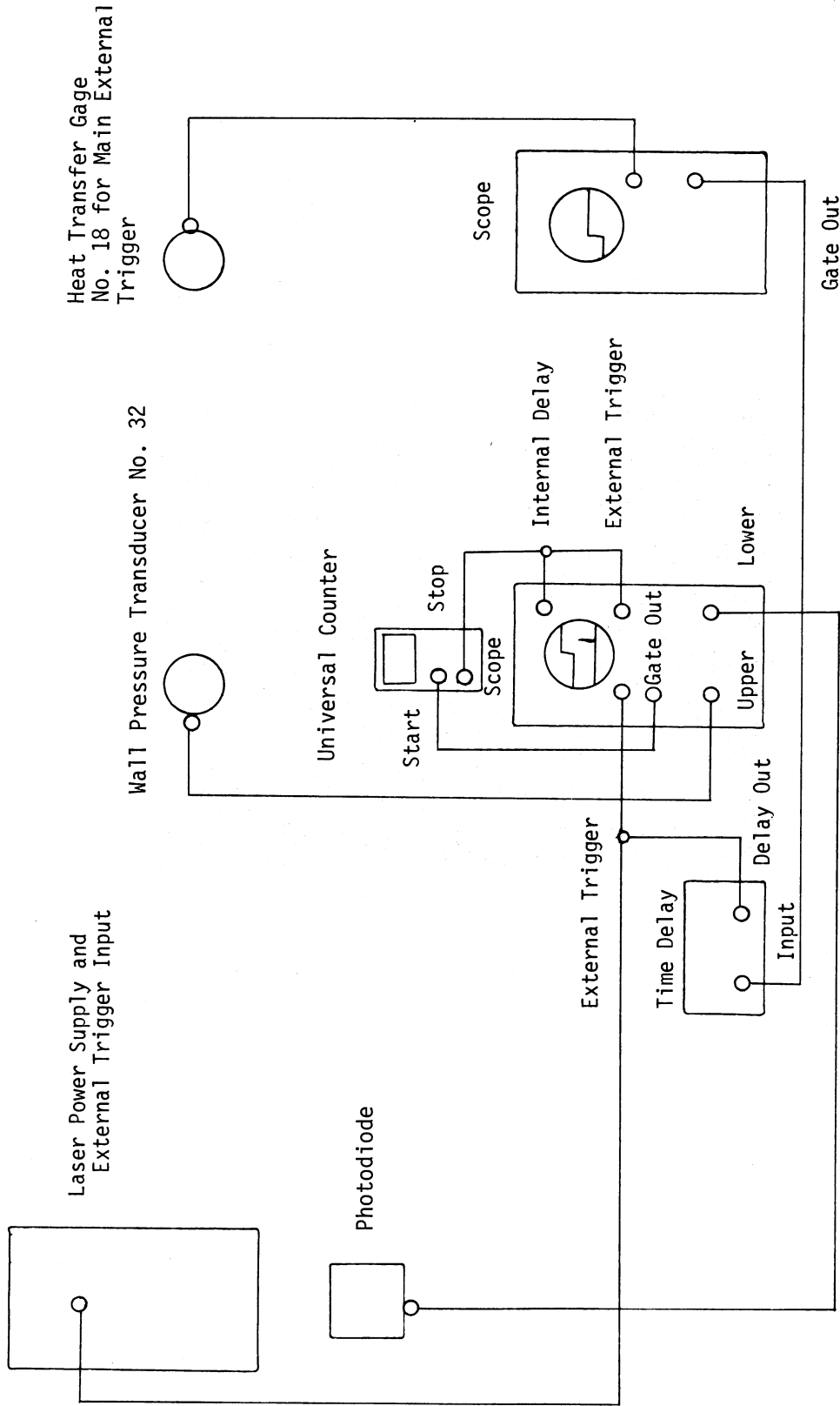
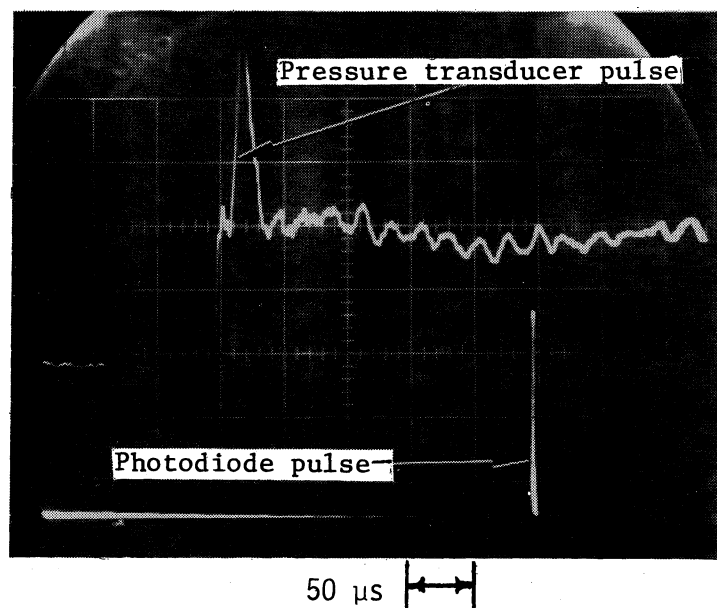
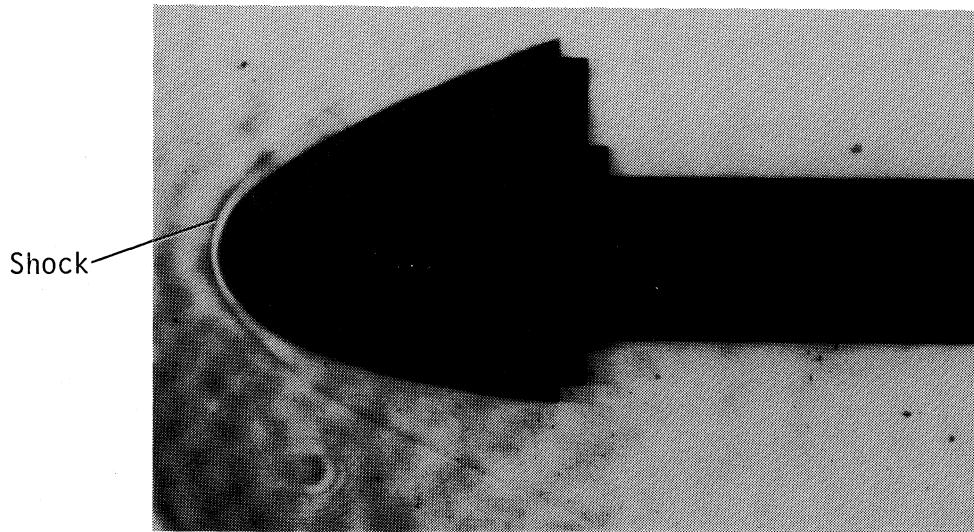


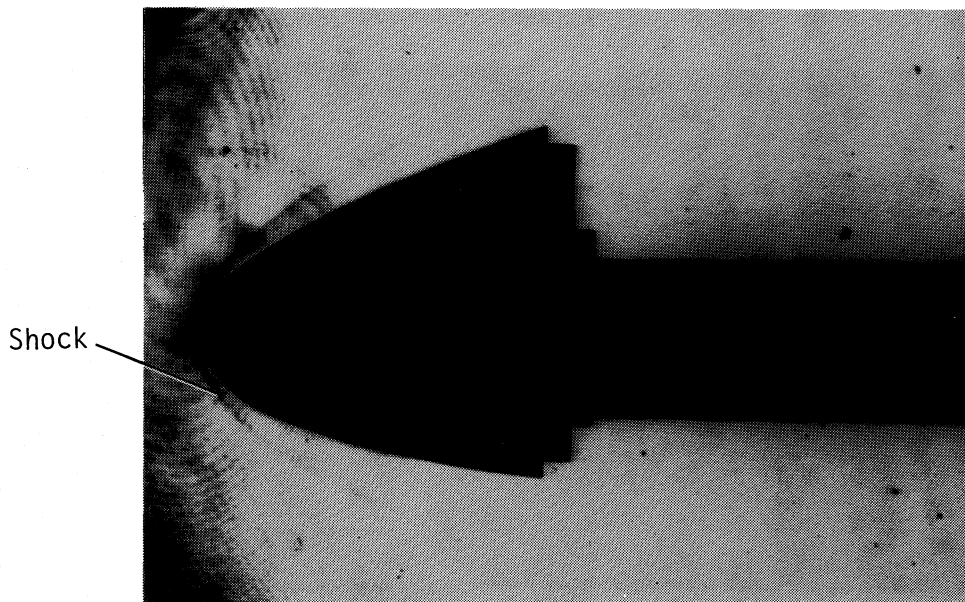
Figure 5.- Ruby-laser timing and recording system at expansion tube.



L-81-129
Figure 6.- Wall pressure gage no. 32 and laser photodiode trace typical of expansion-tube-run data. Laser pulse fired 250 μ s after flow on model.

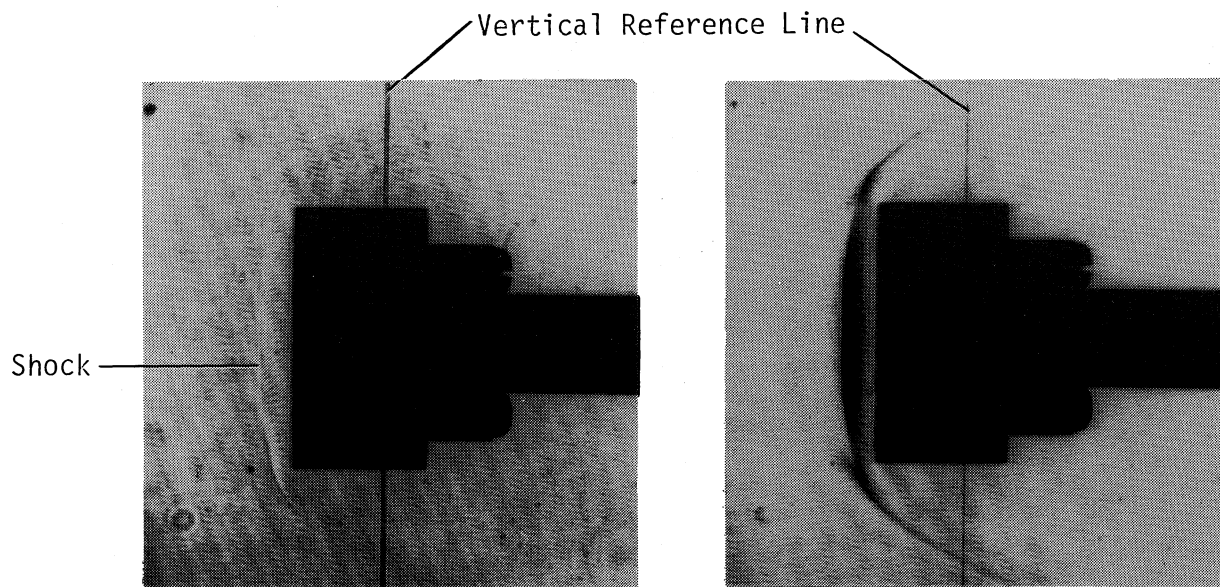


(a) Laser schlieren.



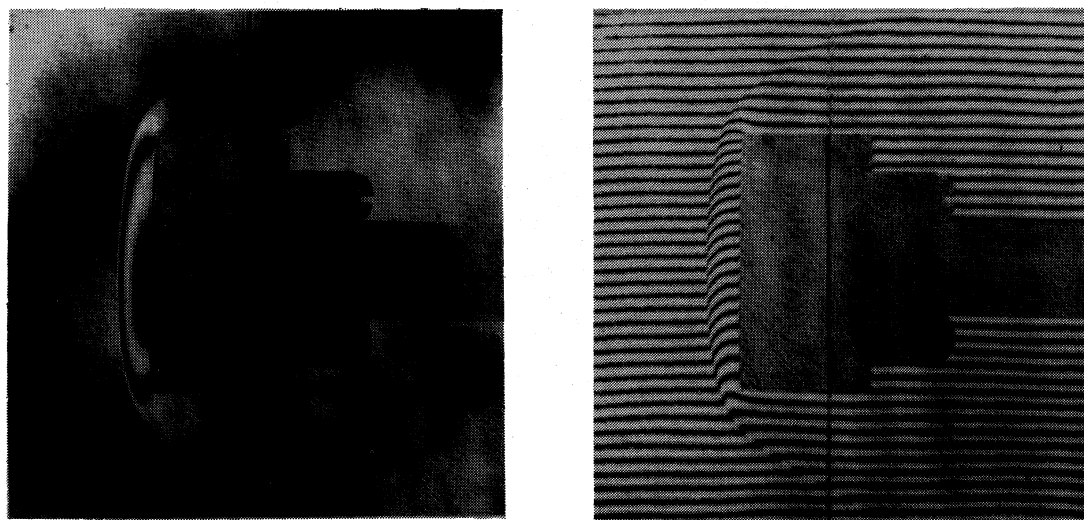
(b) Holographic schlieren.

L-81-130
Figure 7.- Comparisons of simultaneous recordings of laser schlieren and holographically reconstructed schlieren of the Space Shuttle Orbiter nose tip in a test gas of air. $U_{\infty} = 5.3 \text{ km/s}$; $M_{\infty} = 7.6$; $\rho_{\infty} = 0.006 \text{ kg/m}^3$; $\Delta\rho = 0.062 \text{ kg/m}^3$.



(a) Shadowgraph.

(b) Schlieren.

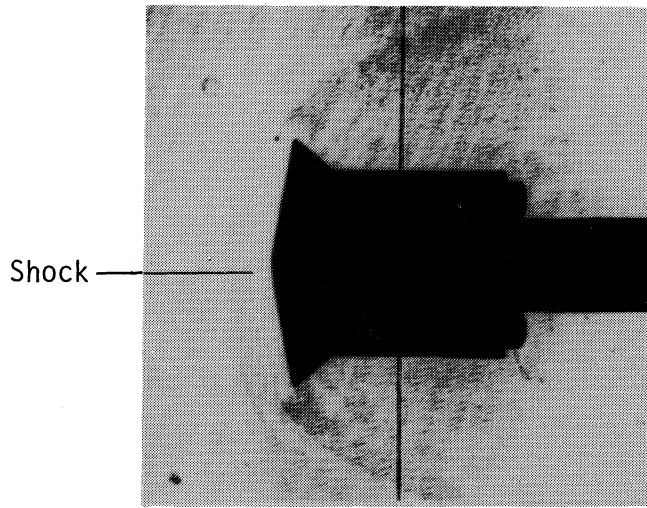


(c) Infinite-fringe interferogram.

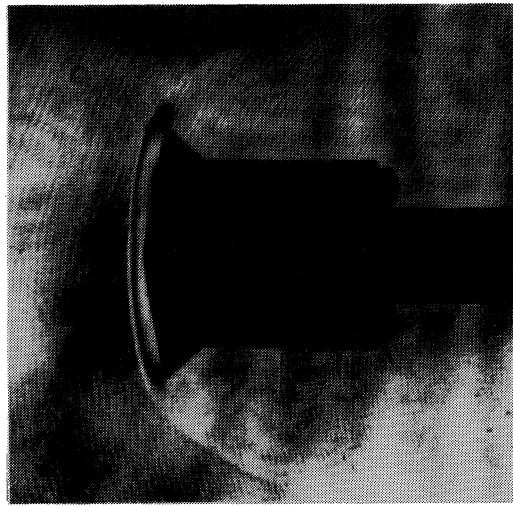
(d) Finite-fringe interferogram.

L-81-131

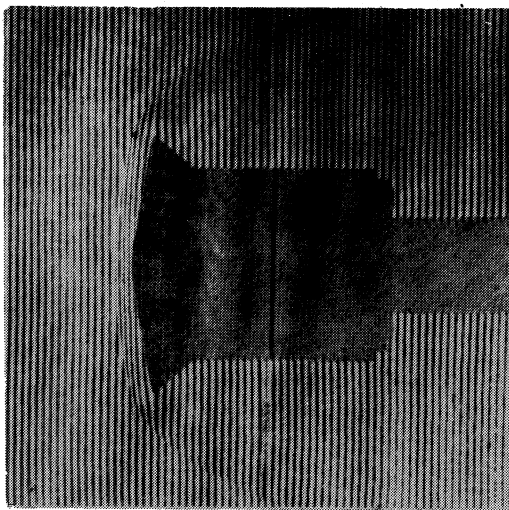
Figure 8.- Holographic reconstructions from a run in Langley Expansion Tube with flat-faced cylinder model in a test gas of CO_2 . $U_\infty = 5.02 \text{ km/s}$; $M_\infty = 9.8$; $\rho_\infty = 0.0053 \text{ kg/m}^3$; $\Delta\rho = 0.0950 \text{ kg/m}^3$.



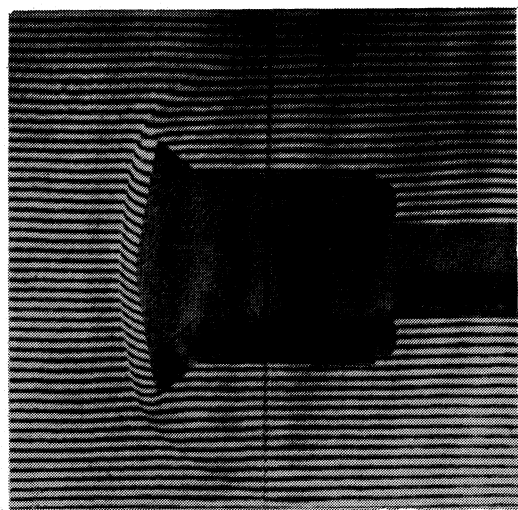
(a) Shadowgraph.



(b) Infinite-fringe interferogram.



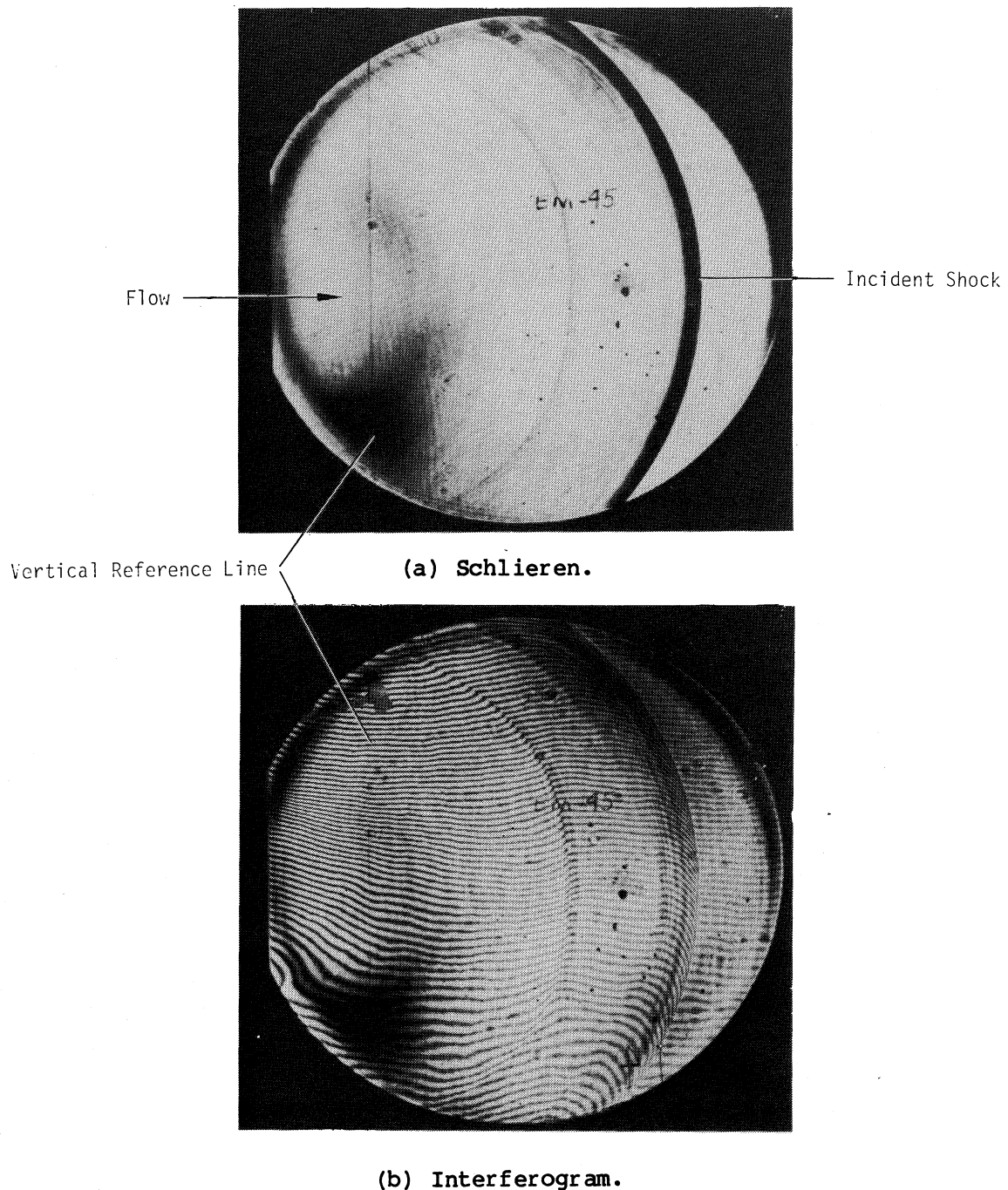
(c) Vertical reference-fringe interferogram.



(d) Horizontal reference-fringe interferogram.

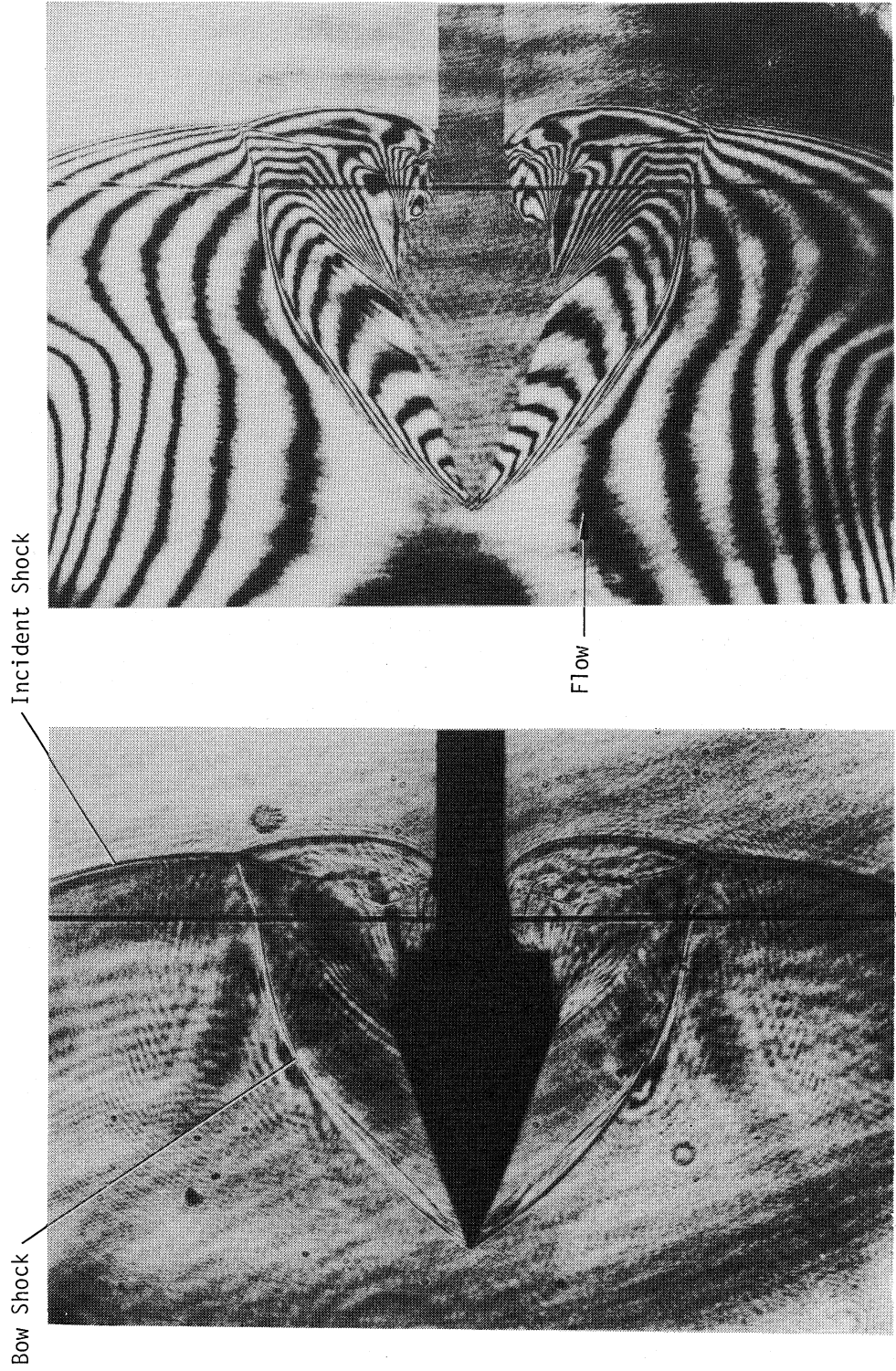
L-81-132

Figure 9.- Holographic reconstructions of a spherically blunted, 80° half-angle-cone model from a run in Langley Expansion Tube with test gas of CO_2 . $U_\infty = 5.03 \text{ km/s}$; $M_\infty = 9.8$; $\rho_\infty = 0.0053 \text{ kg/m}^3$; $\Delta\rho = 0.0950 \text{ kg/m}^3$.



L-81-133

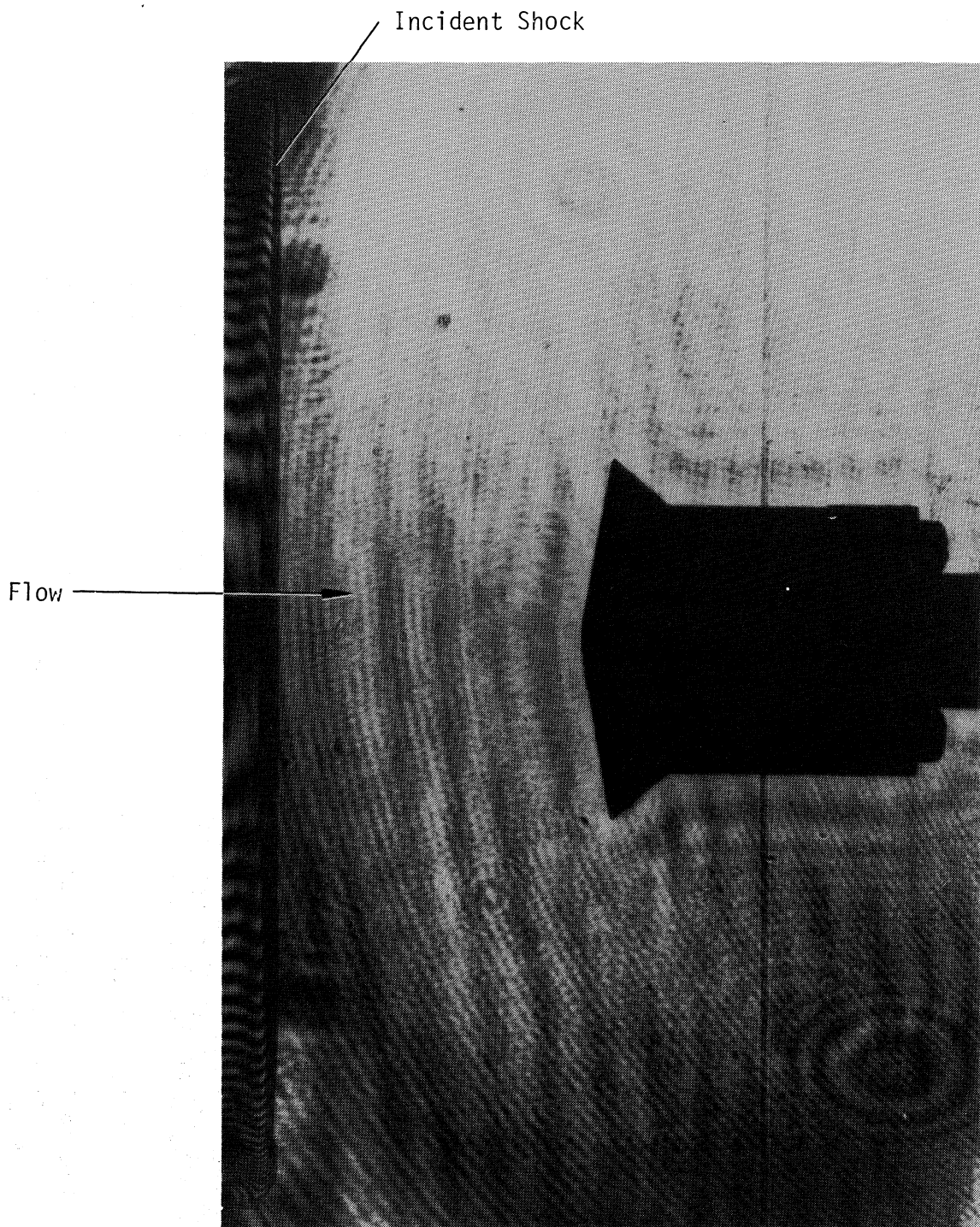
Figure 10.- Two-plate holography with Langley Expansion Tube operated as a shock tube illustrating incident shock wave following exit from the tube. The test gas used was argon. $U_{S,1} = 2.54$ m/s; $M_{S,1} = 7.9$; $\Delta\rho = 0.21$ kg/m³.



(a) Shadowgraph.

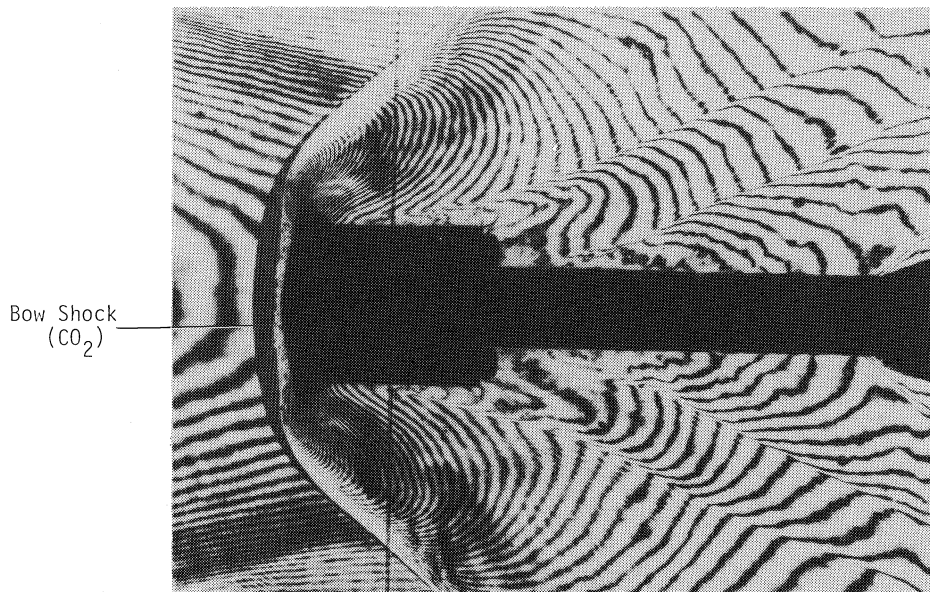
(b) Interferogram.

Figure 11.- Two-plate holography of a shock tube run with 200 half-angle-wedge model with air as test gas. $U_{s,1} = 2.29$ km/s; $M_{s,1} = 6.7$; $\Delta\rho = 0.23$ kg/m³. L-81-134

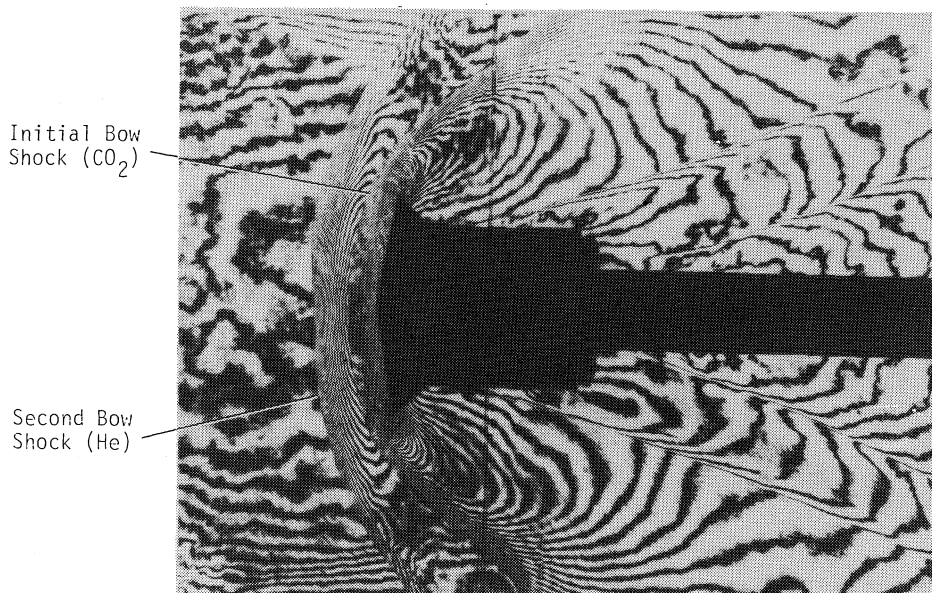


L-81-135

Figure 12.- Double-pulse holographic interferogram of shock exiting tube before it has impacted blunted 80° half-angle-cone model. The test gas used was CO_2 . $U_{S,1} = 2.47 \text{ km/s}$; $M_{S,1} = 9.0$; $\Delta\rho = 0.72 \text{ kg/m}^3$.



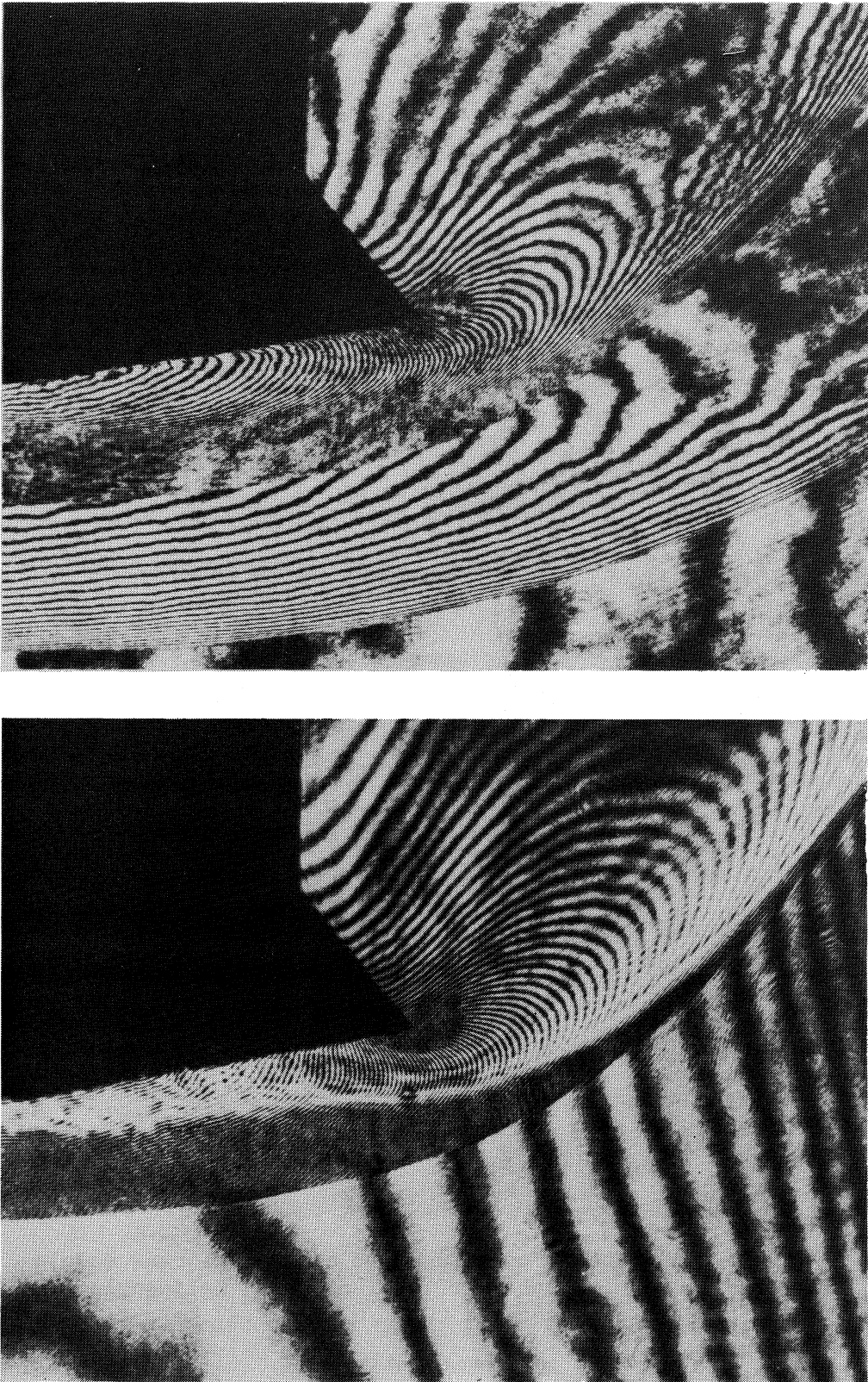
(a) First pulse before flow and second pulse during flow.



(b) Both pulses during flow.

L-81-136

Figure 13.- Double-pulse inteferograms of two shock-tube runs made under same conditions of a spherically blunted 80° half-angle-cone model. The test gas used was CO_2 . $U_{S,1} = 2.47 \text{ km/s}$; $M_{S,1} = 9.0$; $\Delta\rho = 4.0 \text{ kg/m}^3$.



(a) First pulse before flow and second pulse during flow.

(b) Both pulses during flow.

Figure 14.- Magnification (50x) of interferograms of figure 13.

L-81-137

1. Report No. NASA TM-83116		2. Government Accession No.		3. Recipient's Catalog No.	
4. Title and Subtitle HOLOGRAPHIC FLOW VISUALIZATION AT THE LANGLEY EXPANSION TUBE				5. Report Date June 1981	
				6. Performing Organization Code 506-51-23-02	
7. Author(s) William K. Goad and Alpheus W. Burner				8. Performing Organization Report No. L-14410	
				10. Work Unit No.	
9. Performing Organization Name and Address NASA Langley Research Center Hampton, VA 23665				11. Contract or Grant No.	
				13. Type of Report and Period Covered Technical Memorandum	
12. Sponsoring Agency Name and Address National Aeronautics and Space Administration Washington, DC 20546				14. Sponsoring Agency Code	
15. Supplementary Notes					
16. Abstract <p>A holographic system used for flow visualization at the Langley Expansion Tube is described. A ruby laser which can be singly or doubly pulsed during the short run time of less than 300 μs is used as the light source. With holography, sensitivity adjustments can be optimized after a run instead of before a run as with conventional flow-visualization techniques. This results in an increased reliability of the flow visualization available for the study of real-gas effects on flow about models. Holographic techniques such as single-plate schlieren and shadowgraph, two-plate interferometry, double-pulse interferometry for "perfect" infinite-fringe interferograms, and double-pulse interferometry used to examine changes in the flow over a short time period are described and examples presented.</p>					
17. Key Words (Suggested by Author(s)) Holographic interferometry Laser Flow visualization Hypersonic-hypervelocity flows Shock tube			18. Distribution Statement Unclassified - Unlimited Subject Category 35		
19. Security Classif. (of this report) Unclassified		20. Security Classif. (of this page) Unclassified		21. No. of Pages 22	22. Price A02

For sale by the National Technical Information Service, Springfield, Virginia 22161

NASA-Langley, 1981